

Adaptive Engagement Control of a Self-Energizing Clutch Actuator System Based on Robust Position Tracking

Jinsung Kim¹, Member, IEEE, Seibum B. Choi², Member, IEEE, and Jiwon J. Oh¹

Abstract—This paper considers the problem of designing an engagement controller for a clutch actuator system having a self-energizing mechanism. Since such a system includes a torque amplification mechanism, parametric uncertainties in the model may lead to large erroneous results in the clutch torque controller. To compensate this undesirable effect, adaptive sliding-mode control is applied based on the actuator position tracking. Estimations of the disk friction coefficient and actuator motion parameters are employed to control the engagement torque properly. The disk friction coefficient adaptation provides online stiffness inference for the engagement force while in contact. Moreover, the unstructured disturbance is also compensated by a disturbance observer. Experimental verifications show the improved performance of the developed control method.

Index Terms—Adaptive control, automotive system, clutch actuator, drivetrain, positioning mechanism, torque control.

I. INTRODUCTION

RECENTLY, automotive engineering technology related to the improvement of fuel efficiency has received much attention. As a solution to this problem, advanced automotive transmissions have been developed. Due to the better efficiency, automated manual transmissions (AMTs) and dual-clutch transmissions (DCTs) have attracted considerable attention of automotive manufacturers. Unlike traditional automatic transmissions that guarantee smooth transient responses by a torque converter, AMTs and DCTs should consider clutch control performance because a friction clutch directly connects the engine and transmissions without a torque converter. In these systems, the clutch and the gear-shifting mechanism are generally operated by electrical or hydraulic actuators. There are several control issues to meet performance requirements in order to automate operation via the servoactuated system.

Manuscript received January 29, 2017; revised May 22, 2017; accepted January 1, 2018. Date of publication January 15, 2018; date of current version April 16, 2018. Recommended by Technical Editor J. Wang. (Corresponding author: Jinsung Kim.)

J. Kim and J. J. Oh are with Hyundai Motor Company, Hwasung 18280, South Korea (e-mail: jsk@kaist.ac.kr; jwo@kaist.ac.kr).

S. B. Choi is with the Department of Mechanical Engineering, Korea Advanced Institute of Science and Technology, Daejeon 34141, South Korea (e-mail: sbchoi@kaist.ac.kr).

Color versions of one or more of the figures in this paper are available online at <http://ieeexplore.ieee.org>.

Digital Object Identifier 10.1109/TMECH.2018.2793351

One of the major issues in automotive clutch systems is the torque control. Usually, an indirect approach for control should be required, since the use of clutch torque measurement by a sensor is prohibitively expensive. Also, it should be noted that the torque transmission capability of the clutch varies with temperature, humidity, and friction materials.

When the controller is designed without considering model uncertainties and external disturbances, excessive clutch slip or overactuation may always occur. Furthermore, when the system is equipped with a dry clutch, it is particularly problematic due to the nonlinear nature of dry friction behavior.

Many control methods have been studied for dry clutch engagement. Those control strategies include a decoupled proportional–integral-type controller [1], a linear quadratic regulator, [2]–[6], a backstepping technique [7], [8], model reference adaptive control [9], and model-predictive control [10]. For the study of a torque transmissibility, a dynamic model of clutch temperature has been established in [11]. A clutch torque estimator has been designed in order to compensate the modeling uncertainties [12], [13].

Since a clutch torque is sensitive to corresponding actuator stroke, actuator dynamic behavior and physical limitations should be considered to improve the transient performance [14]. For this reason, several recent studies have investigated the control method of automotive clutch actuator systems for the hydraulic actuator [15]–[20], an electropneumatic actuator [21], [22], and electromechanically driven clutch actuators with dry clutch [23], [24].

Recently, a self-energizing clutch actuator (SECA) system that utilizes the self-energizing effect to reinforce the clutch normal force is proposed [13], [25]–[27]. The operation principle of the SECA system has been introduced in [26], where it only shows the validation of self-energizing effect at the newly designed clutch setup. In [13], the clutch torque observer based on the reaction torque estimation has been proposed for accurate torque monitoring.

In this paper, we propose the development of a clutch torque controller for the SECA system. Since such systems include a torque amplification mechanism, parametric uncertainties in the actuator model yield large erroneous results in the clutch torque feedback controller. Thus, a clutch positioning controller should be designed to be robust against torque amplification characteristics.

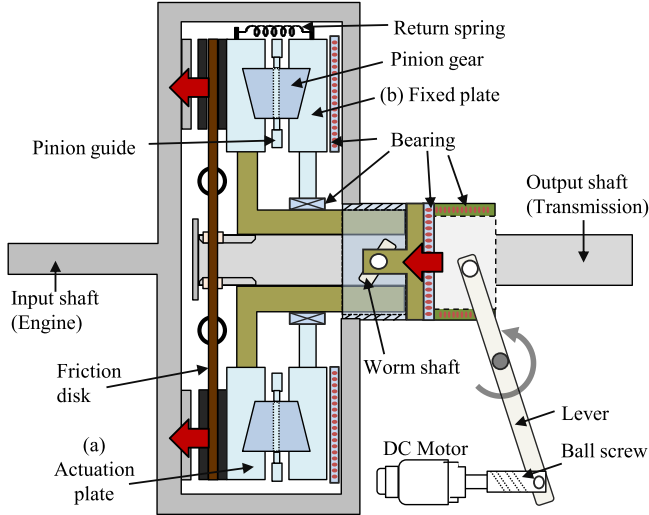


Fig. 1. Schematic of a SECA.

The main strategy is to employ adaptive sliding-mode control (ASMC) with parameter adaptation of the friction coefficient on the clutch disk surface during the slip phase. In addition, a disturbance observer (DOB) is incorporated with ASMC to enhance robustness of the overall control system. The settling time can be reduced by the help of the DOB.

In the literature, the DOB approach is combined with other robust control methods. Sliding-mode control (SMC) with DOB compensation can alleviate the chattering associated with the switching gain [28], [29]. The combination of a DOB and parameter adaptation is proposed in order for robustness enhancement with respect to input-to-state stability sense [30].

In the overall design framework, while a DOB is incorporated as a means to estimate and cancel unknown compounded disturbance at a low-frequency range, ASMC compensates parametric uncertainties in high frequencies effectively. Unlike [30], the stability of the combined system in this research is proved by the Lyapunov-based analysis. The resulting sufficient condition can provide a straightforward way to select the bandwidth parameter of the DOB.

By monitoring the disk friction coefficient using an adaptive mechanism, the controller is guaranteed to track the desired torque trajectory asymptotically despite the presence of parametric uncertainties on the actuator system. Also, the motion friction parameters are estimated to improve the tracking accuracy with the slight modification of the modeling compared with [26].

The rest of this paper is organized as follows. In Section II, the brief description and the dynamic model of the system are introduced. In Section III, a clutch torque controller based on the position control is designed. Experimental validations are given in Section IV, and conclusions can be found in Section V.

II. SYSTEM AND MODEL

The schematic of the SECA system is shown in Figs. 1 and 2. In this paper, since we focus on the adaptive control of the clutch engagement, refer to the preliminary paper [26] for the

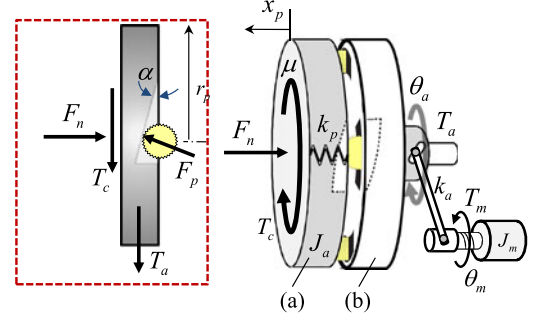


Fig. 2. Equivalent model for a SECA system (a) Actuation plate. (b) Fixed plate.

detailed description of the SECA system. In the following, the full system model and its simplified version are proposed for developing a control-oriented model.

A. Full System Model

1) *Dynamic Model of the Electric Motor:* The dynamic models of the motor are given as follows:

$$L_m \dot{i}_m + R_m i_m + k_m \omega_m = u \quad (1a)$$

$$J_m \dot{\omega}_m + T_{fm}(\omega_m) + \frac{T_a}{N_g} = k_t i_m. \quad (1b)$$

In (1a), u is the voltage applied to the motor, i_m is the motor current, R_m is the resistance, L_m is the inductance, and k_m is the back electromotive force constant. In (1b), J_m is the motor moment of inertia, ω_m is the rotor speed, k_t is the motor torque constant, and N_g is the gear ratio between the motor rotor and the mechanical subsystem. Note that T_a is the load torque for driving the mechanical subsystem that will be introduced in (3). The friction torque T_{fm} in the rotational motion of the motor is described as

$$T_{fm}(\omega_m) = \begin{cases} T_{cm+} + b_m + \omega_m & \omega_m > \epsilon_m \\ T_{cm-} + b_m - \omega_m & \omega_m < -\epsilon_m \\ T_m, & \text{if } |\omega_m| < \epsilon_m \text{ and } |T_{fm}| < T_{fsm} \\ T_{fm} \operatorname{sgn}(T_m), & \text{if } |\omega_m| < \epsilon_m \text{ and } |T_{fm}| > T_{fsm} \end{cases} \quad (2)$$

where T_{cm} is the Coulomb friction torque, b_m is the viscous friction coefficient, and T_{fsm} is the static friction torque. Note that ϵ_m denotes a small zero velocity interval, where the motor velocity is taken into account as zero. The subscripts “+” and “-” are used to represent the hysteresis phenomenon.

2) *Dynamic Model of the Mechanical Subsystem:* The fixed plate shown in Fig. 2 is interposed between the clutch cover and the friction disks in order to adjust the axial displacement of the actuation plate while rotating at the same time. In the clutch open phase, the rotational equation of motion for the actuation plate without the clutch engagement torque is described as

$$J_a \dot{\omega}_a = T_a - T_{fa}(\omega_a) \quad (3)$$

where J_a is the moment of inertia of the actuation plate. Since the pinions are constrained by two supporting plates [(a) and

(b) in Figs. 1 and 2] and the pinion guide, the motion of them coincides with the actuation plate. Thus, it is reasonable to assume that the inertia of the pinions is lumped into that of the actuation plate. The driving torque T_a is generated by an elastic deformation between the motor and the mechanical subsystem with the equivalent torsional stiffness k_a defined as

$$T_a = k_a \left(\frac{\theta_m}{N_g} - \theta_a \right) \quad (4)$$

where θ_m and θ_a are the motor and the actuator angular position, respectively. In (3), the frictional torque T_{fa} on the worm shaft can be represented by replacing the subscript “m” in (2) with “a.”

When the clutch is in contact with the surface for engagement operation, the clutch torque T_c and the reinforcement torque from the interaction force F_p on the rack and pinion surface are added in (3) as shown in Fig. 2. Therefore, the equation of motion for the actuation plate in the slip phase is represented by

$$J_a \dot{\omega}_a = T_a + T_c - 2r_p F_p \sin \alpha - T_{fa}(\omega_a) \quad (5)$$

where r_p is the radius of bevel gear position and α is the inclined surface angle on the actuation plate and the fixed plate. For the positive slip phase, the clutch torque T_c is given as

$$T_c = \mu R_c F_n \quad (6)$$

where, μ is the dry friction coefficient on the disk, R_c is the clutch radius, and F_n is the applied normal force. The interaction force F_p at the contact point between the rack and pinion gear tooth meshed inside the actuation plate depends on the normal force F_n with the inclined surface angle α :

$$F_p = \frac{F_n}{\cos \alpha}. \quad (7)$$

Note that the third term at the right-hand side of (5) is related with a self-energizing effect. The wedge structure comes from the rack and pinion mechanism.

The axial displacement x_p of the actuation plate can be calculated through the geometric relation with the angular position θ_a of that as shown in Fig. 2. It is, therefore, given by $x_p = \beta \theta_a$ with

$$\beta \triangleq 2r_p \tan \alpha. \quad (8)$$

The normal force applied on the friction disk is

$$F_n = k_p x_p = k_p \beta \theta_a \quad (9)$$

where k_p is the stiffness of the actuation plate. It is assumed that the normal force F_n is proportional to the actuator stroke x_p in the axial direction.

According to (7) and (9), the actuator dynamics (5) in the positive slip phase can be rewritten as

$$J_a \dot{\omega}_a = \mu R_c F_n + T_a - \beta F_n - T_{fa}(\omega_a, z_a). \quad (10)$$

Overall system dynamics described in this section is shown in Fig. 3.

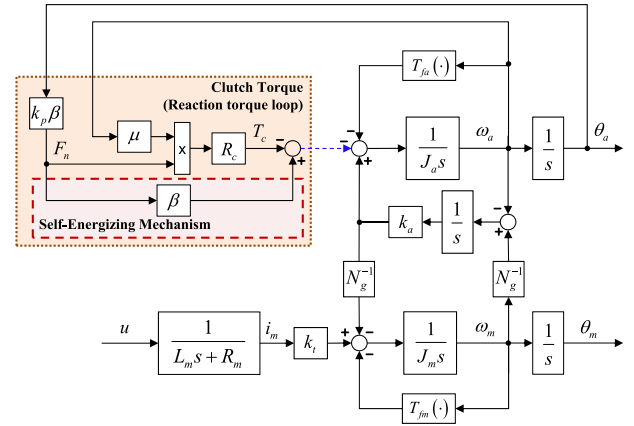


Fig. 3. Block diagram of the full model for a clutch actuator system introduced in Section II-A [β is defined in (8)].

B. Simplified Model for Control

In order to facilitate a control design and implementation, the order of the system model is reduced by neglecting high-frequency components. The following assumptions are made to simplify the actuator model.

- A1) The electrical dynamics of the dc motor is faster than the mechanical motion.
- A2) The bandwidth of the actuation plate motion is very high, and its rotating angle is very small.
- A3) In the mechanical subsystem, frictional motion during presliding can be negligible [31].

A1 means that the inductance of the dc motor could be neglected, by which L_m is much smaller than J_m [32]. Thus, the dynamic equation (1a) is converted into an algebraic equation as follows:

$$u = R_m i_m + k_m \omega_m. \quad (11)$$

Based on A2, the dynamics of the actuation plate is negligible. Consequently, (10) can be rewritten as

$$2r_p F_n \tan \alpha = T_a + \mu R_c F_n. \quad (12)$$

Combining (4) and (12) gives a single equation for the normal force

$$F_n = \frac{k_a (\theta_m / N_g - \theta_a)}{2r_p \tan \alpha - \mu R_c}. \quad (13)$$

Using the normal force expressions (9) and (13), the relationship between the motor angular position and the angular position of the actuation plate is given by

$$\theta_a = \frac{k_a}{N_g (k_b(\mu) + k_a)} \theta_m \quad (14)$$

where the auxiliary function k_b is defined for notational simplicity as

$$k_b(\mu) \triangleq \xi(\mu) (2r_p k_p \tan \alpha) = \xi(\mu) k_p \beta \quad (15a)$$

$$\xi(\mu) \triangleq 2r_p \tan \alpha - \mu R_c = \beta - \mu R_c. \quad (15b)$$

Note that β defined in (8) is determined from a hardware design specification. k_b and ξ in expression (15) are erroneous

parameters due to the friction coefficient μ , which is uncertain and time varying. Equation (14) shows that the positioning of the mechanical subsystem is an uncertain function of the motor position. Substituting (14) into (13) derives the relationship between the clutch normal force and the motor position

$$F_n = \Phi(\mu)\theta_m \quad (16a)$$

$$\Phi(\mu) \triangleq \frac{k_a}{\xi(\mu)} \left[\frac{k_b(\mu)}{N_g (k_b(\mu) + k_a)} \right] \quad (16b)$$

where the nonlinear function $\Phi(\mu)$ is nonsingular because all parameters in (16b) are bounded. The above equation is applied to convert the desired normal force to the desired motor position, which will be used in the subsequent control development.

From A3, the following linear-in-parameters model for motion friction depending only on the velocity is given by

$$T_f(\omega_m) = \phi_1 \text{sgn}(\omega_m) + \phi_2 \omega_m \\ \phi_1 \triangleq \sigma_0 g(\omega_m), \quad \phi_2 \triangleq \sigma_2 \quad (17)$$

where σ_0 and σ_1 are dominant friction parameters in the simplified model. The detailed simplification process can be found in [31]. Actual values of friction parameters are unknown but bounded.

Combining (1b), (11), (12), (14), and (17) yields

$$\bar{J}_m \dot{\omega}_m + q\omega_m + T_f(\omega_m) + r(\mu)\theta_m = p(u + d) \quad (18)$$

where \bar{J}_m in (19a) and r in (19d) are the equivalent moment of inertia and the nonlinear function of the friction coefficient, respectively. Note that d is the unstructured disturbance from the unmodeled effect and the model reduction. It can be decomposed into d_h in high frequencies and d_l in low frequencies. They are assumed to be bounded. For simplicity, other auxiliary variables p , q , and w are defined as

$$\bar{J}_m \triangleq J_m + \frac{J_a}{N_g}, \quad w \triangleq \frac{k_a}{N_g^2} \quad (19a)$$

$$p \triangleq \frac{k_t}{R_m} \quad (19b)$$

$$q \triangleq \left(\frac{k_t k_m}{R_m} + b_m \right) \quad (19c)$$

$$r(\mu) \triangleq \frac{k_a k_b(\mu)}{N_g^2 [k_b(\mu) + k_a]} = w \left(\frac{k_b(\mu)}{k_b(\mu) + k_a} \right) \quad (19d)$$

$$d = d_h + d_l. \quad (19e)$$

As a result, the reduced order model can be expressed as a second order. The fourth term implicitly includes the engagement torque when the clutch is in contact. The problem might appear to be one of the position tracking problems with uncertain reaction torque corresponding to the equivalent reaction load $r(\mu)\theta_m$.

III. CLUTCH ENGAGEMENT CONTROL DEVELOPMENT

The overall control system for the clutch engagement has two subcontrollers in a large point of view. First, the ASMC is used to satisfy a desired performance specification and to

compensate structured uncertainties for a linear-in-parameters form especially in the high-frequency range. The disk friction coefficient is estimated to improve the control accuracy when the clutch comes into contact. Second, as an inner-loop compensator, the DOB compensates the unmodeled effect and unstructured disturbances at low frequencies. Therefore, it can reduce uncertainties in the input channel by rejecting the unknown disturbances.

A. Problem Formulation

The objective of the proposed strategy is to design a clutch normal force tracking controller. Due to the presence of nonlinear friction and parametric uncertainties, a robust control method is required to meet the desired specification. However, since torque transducers are very expensive, the clutch torque measurement is impractical for real environment.

On the other hand, the motor position can be measured easily using an incremental encoder. And, the clutch torque/force is converted into the actuator stroke by the relationship between the normal force and the motor position in (16a). It can be expressed as a nonlinear function of the motor position by $\Phi(\mu)$ defined in (16b). Therefore, the motor position error will be used to define a sliding surface instead of the normal force.

Let $e_f \triangleq F_{nd} - F_n$ be the normal force tracking error with the desired normal force F_{nd} . The motor position error e_m is defined as $e_m \triangleq \theta_{md} - \theta_m$ and its derivative $\dot{e}_m = \dot{\theta}_{md} - \dot{\theta}_m$. By using (16), it can be also represented as

$$e_m = \Phi^{-1}(\mu)e_f. \quad (20)$$

Then, the filtered tracking error z is defined as

$$z \triangleq \dot{e}_m + \lambda e_m \quad (21)$$

where, λ is a constant design parameter.

The following open-loop error system is obtained by multiplying \bar{J}_m on the time derivative of (21) and combining (18):

$$\bar{J}_m \dot{z} = \phi_1 \omega_m + \phi_2' \omega_m + r(\mu)\theta_m + \bar{J}_m \dot{\omega}_m - p(u + d_h + d_l) \quad (22)$$

where $\dot{\omega}_m := \ddot{\theta}_{md} + \lambda \dot{e}_m$ and $\phi_2' = \phi_2 + q$.

B. Adaptive Sliding Control Design

Since the self-energizing characteristics of the given system can amplify the applied normal force, small parametric uncertainty may lead to the significant tracking error that implies the mismatch between the desired force and the actual one [27].

Another drawback is mechanical design complexity induced by actual implementation of the self-energizing mechanism. This problem also leads to highly nonlinear friction disturbances during operation. In order to overcome this problem, SMC is first introduced to make a control system robust against unmodeled dynamics and effective tracking capability. In addition, it is necessary to account for the motion friction compensation by parameter adaptation to alleviate high control action of SMC.

Also, the disk friction coefficient μ is an uncertain parameter. It varies with the operating temperature, material properties, and a slip speed of both sides of the clutch. To compensate this

uncertainty, an adaptation scheme for the disk friction coefficient μ will be designed later.

The control law (22) based on ASMC is defined as

$$u = \frac{1}{p} (u_r + M \operatorname{sgn}(z)) + u_d \quad (23)$$

$$\text{where } u_r = u_0 + u_{a1} + u_{a2} \quad (24a)$$

$$u_0 = Kz + \bar{J}_m \dot{\omega}_{mr} \quad (24b)$$

$$u_{a1} = \hat{r} \theta_m \quad (24c)$$

$$u_{a2} = \hat{\phi}_1 \operatorname{sgn}(\dot{\theta}_m) + \hat{\phi}_2' \dot{\theta}_m \quad (24d)$$

$$u_d = -\hat{d}_l \quad (24e)$$

where u_0 is a feedback controller including feedforward action, u_{a1} is the adaptive controller for the motion tracking, and u_{a2} is the adaptive disk friction compensator. In particular, u_d is the disturbance compensator to be synthesized in Section III-D. \hat{r} , \hat{k}_b , and $\hat{\mu}$ are estimated parameters of r , k_b , and μ , respectively. \hat{r} and \hat{k}_b are also defined as

$$\hat{r} \triangleq r(\hat{\mu}) = w \left(\frac{\hat{k}_b(\hat{\mu})}{\hat{k}_b(\hat{\mu}) + k_a} \right) \quad (25)$$

$$\hat{k}_b \triangleq \xi(\hat{\mu}) k_p \beta. \quad (26)$$

Here, \hat{r} includes an erroneous parameter \hat{k}_b , which is a function of $\hat{\mu}$ and other system parameters. The closed-loop system is rewritten by substituting (23) into (22) as

$$\begin{aligned} \bar{J}_m \dot{z} = & \tilde{q} \dot{\theta}_m + \tilde{\phi}_1 \operatorname{sgn}(\dot{\theta}_m) + \tilde{\phi}_2' \dot{\theta}_m + \tilde{r} \theta_m \\ & - Kz - M \operatorname{sgn}(z) - p \tilde{d}_l + p d_h \end{aligned} \quad (27)$$

where $\tilde{r} = r(\mu) - \hat{r}(\hat{\mu})$, $\tilde{\phi}_1 = \phi_1 - \hat{\phi}_1$, and $\tilde{\phi}_2' = \phi_2' - \hat{\phi}_2'$ are the parameter estimation errors. The disturbance estimation error is denoted as $\tilde{d}_l = d_l - \hat{d}_l$. Note that \tilde{r} is a function of various parameters including parameter uncertainty of μ , as shown in (25).

C. Adaptation Laws

The disk friction coefficient adaptation requires an additional assumption that is trivial during the clutch slip phase.

A4) The control input can be chosen such that the friction coefficient is within the set Ω_μ

$$\mu \in \Omega_\mu \triangleq \{\mu(\omega_m) \mid \underline{\omega}_m < \omega_m < \bar{\omega}_m\} \quad (28)$$

where $\underline{\omega}_m \triangleq \min_{t \in [0, T]} \omega_m$, $\bar{\omega}_m \triangleq \max_{t \in [0, T]} \omega_m$.

A4 says that the friction coefficient μ on the clutch disk surface is confined to the range of (28). It implies that the actuator rotational speed is not a constant ensuring that the persistence excitation (PE) condition for parameter adaptation is satisfied. Equation (28) defines a validity domain of the estimation for the disk friction coefficient. Note that A4 is generally met when the clutch slip remains.

The sliding control input in (23) plays a crucial role in satisfying A4. Due to the limitation of actuator bandwidth, the

sign function is approximated by a saturation function that is defined as

$$\operatorname{sat}(z) = \begin{cases} \frac{z}{\sigma}, & \text{if } |z| \leq \sigma \\ \frac{z}{|z| + \delta}, & \text{otherwise} \end{cases} \quad (29)$$

where $\sigma > 0$ denotes the switching boundary and $\delta > 0$ denotes the approximation margin. A continuous slip of the clutch depends on the switching frequency of the control signal resulting from the selection of both parameters σ and δ . The finite switching of (29) could intentionally induce a clutch slip to identify the friction coefficient.

In the subsequent development, adaptation laws are updated depending on the tracking error so that a small control error may exhibit parameter drifting. It should be noted that adaptation laws keep the estimate of the friction coefficient within the physical boundary.

To do this, the projection operator for a given vector $\hat{\chi}$ needs to be defined. Let $\mathcal{P} := \{r \in \mathbb{R} \mid \kappa \leq 0\}$ be a closed convex set and $\kappa \in \mathbb{R}^p$ a smooth function. The projection operator is defined as

$$\begin{aligned} \operatorname{Proj}_{\hat{\chi}}(\zeta) &= \begin{cases} \zeta, & \text{if } \hat{\chi} \in \mathcal{P}^0 \text{ or if } \nabla \kappa^T \zeta \geq 0 \\ \left(1 - \varepsilon \frac{\nabla \kappa \nabla \kappa^T}{\nabla \kappa^T \varepsilon \nabla \kappa}\right) \zeta, & \text{if } \hat{\chi} \in \partial \mathcal{P} \text{ and } \nabla \kappa^T \zeta < 0 \end{cases} \end{aligned}$$

where $\zeta \in \mathbb{R}^p$ is any adaptive function, $\varepsilon \in \mathbb{R}^{p \times p}$ is a positive-definite adaptive gain matrix, \mathcal{P}^0 is the interior of \mathcal{P} , $\partial \mathcal{P}$ is the boundary of \mathcal{P} , and $\nabla \kappa = d\kappa/d\hat{\chi}$ is the outward unit normal vector at $\hat{\chi} \in \partial \mathcal{P}$. With the prior knowledge of the parameter variation range, a projection operator plays the role of preserving the passivity property of a self-energizing effect.

Let the admissible region $\mathcal{P}_{\hat{\mu}}$ be a closed set given as $\mathcal{P}_{\hat{\mu}} := \{\hat{r} \in \mathbb{R} \mid \xi(\hat{\mu}) > 0\}$, where the clutch does not get stuck [26]. The adaptive law of \hat{r} is designed by

$$\begin{aligned} \dot{\hat{r}} &= \operatorname{Proj}(\varepsilon \theta_m z) \\ &= \begin{cases} \varepsilon \theta_m z, & \text{if } \hat{r} \in \mathcal{P}_{\hat{\mu}}^0 \text{ or if } \nabla \kappa_{\hat{\mu}}^T \varepsilon \theta_m z \geq 0 \\ 0, & \text{otherwise} \end{cases} \\ \hat{r}(0) &= r_0 \end{aligned} \quad (30)$$

where r_0 is a prescribed nominal value of r . The solution trajectory of (30) is confined within $\Omega_{\hat{r}} = \{\hat{r} \leq \hat{r} \leq \bar{r}\} \subset \mathcal{P}_{\hat{\mu}}^0$. Equation (30) is also valid to ensure that \hat{k}_b makes its estimate stay in the region $\mathcal{P}_{\hat{\mu}}$. It can be shown as follows. Since β and k_p are positive constants in (15), \hat{k}_b is also positive when $\xi(\hat{\mu})$ is a positive function. With this and the fact

$$\frac{\partial \hat{r}}{\partial \hat{k}_b} = w \frac{k_a}{(\hat{k}_b + k_a)^2} > 0 \quad (31)$$

it implies that \hat{r} is positive when $\xi(\hat{\mu}) > 0$. As a result, \hat{r} is evolved inside $\mathcal{P}_{\hat{\mu}}$ or along the tangential plane of $\partial \mathcal{P}_{\hat{\mu}}$. Note that \hat{r} can be assumed as a slowly varying parameter so that the time derivative becomes $\dot{\hat{r}}_n = -\hat{r}_n$. Adaptation laws for compensating nonlinear friction in motion in the system are

given with initial conditions $\hat{\phi}_1(0)$ and $\hat{\phi}_2(0)$ as

$$\dot{\hat{\phi}}_1 = \text{Proj} \left(\delta_1 \text{sgn}(\dot{\theta}_m) z \right), \quad \hat{\phi}_1(0) = f_s \quad (32)$$

$$\dot{\hat{\phi}}_2 = \text{Proj} \left(\delta_2 \dot{\theta}_m z \right), \quad \hat{\phi}_2(0) = b_m \quad (33)$$

where δ_1 and δ_2 are design parameters for determining the adaptation rate.

Theorem 1: Assume that the unstructured uncertainties at a low frequency d_l is not considered in the tracking error system (22), i.e., $d_l = 0$. Under the assumptions A1–A4, the controller given by (23) in conjunction with the adaptation laws (30), (32), and (33) ensures the asymptotic tracking of the normal force control system in the sense that

$$\tilde{\theta}_m \rightarrow 0 \quad \text{and} \quad \text{as} \quad t \rightarrow \infty$$

and the disk friction coefficient error converged to zero in a given compact set μ in $\Omega_\mu \times \mathcal{P}_\mu$ provided that $\varepsilon > 0$, $\delta_1 > 0$, and $\delta_2 > 0$ are properly chosen, and the desired trajectory θ_{md} is sufficiently bounded and smooth (i.e., $\theta_{md}, \dot{\theta}_{md}, \ddot{\theta}_{md} \in \mathcal{L}_\infty$).

Proof: Let $V(z, \tilde{r}, \tilde{\phi}_1, \tilde{\phi}_2) \in \mathbb{R}$ denote a positive-definite Lyapunov function candidate

$$V = \frac{1}{2} \bar{J}_m z^2 + \frac{1}{2\varepsilon} \tilde{r}^2 + \frac{1}{2\delta_1} \tilde{\phi}_1^2 + \frac{1}{2\delta_2} \tilde{\phi}_2^2 \quad (34)$$

and the time derivative of (34) along the trajectory of (27) with $\tilde{d} = 0$ is given by

$$\dot{V} = \bar{J}_m z \dot{z} + \frac{1}{\varepsilon} \tilde{r} \dot{\tilde{r}} + \frac{1}{\delta_1} \dot{\tilde{\phi}}_1^2 + \frac{1}{\delta_2} \dot{\tilde{\phi}}_2^2. \quad (35)$$

Using (23) and (27), it is rewritten as

$$\begin{aligned} \dot{V} &= z [\tilde{\phi}_1 \text{sgn}(\dot{\theta}_m) + \tilde{\phi}_2 \dot{\theta}_m + \tilde{r} \theta_m - Kz \\ &\quad - pd_h - M \text{sgn}(z)] - \frac{1}{\varepsilon} \tilde{r} \dot{\tilde{r}} - \frac{1}{\delta_1} \tilde{\phi}_1 \dot{\tilde{\phi}}_1 - \frac{1}{\delta_2} \tilde{\phi}_2 \dot{\tilde{\phi}}_2 \\ &= -Kz^2 + pd_h z - M|z| + \tilde{r} \left[\theta_m z - \frac{\dot{\tilde{r}}}{\varepsilon} \right] \\ &\quad + \tilde{\phi}_1 \left[\text{sgn}(\dot{\theta}_m) z - \frac{\dot{\tilde{\phi}}_1}{\delta_1} \right] + \tilde{\phi}_2 \left[\theta_m z - \frac{\dot{\tilde{\phi}}_2}{\delta_2} \right] \end{aligned} \quad (36)$$

where the design parameter M is selected to satisfy the inequality $M \geq |pd_h|$. By utilizing (30), (32), and (33), the following inequality is obtained:

$$\dot{V} \leq -Kz^2. \quad (37)$$

Therefore, the time derivative of V is negative semidefinite. Generally, the control system property of interest is asymptotic stability. Based on (34) and (37), it follows that $z, \tilde{r}, \tilde{\phi}_1, \tilde{\phi}_2 \in \mathcal{L}_\infty$ and $z \in \mathcal{L}_2$. Definition (21) shows that $z \in \mathcal{L}_\infty$ implies $e_m, \dot{e}_m \in \mathcal{L}_\infty$. Equations (30), (32), (33), and projection operators can be used to show that $\hat{r}, \hat{\phi}_1, \hat{\phi}_2 \in \mathcal{L}_\infty$. From these facts, the control inputs (24a)–(24d) are bounded. It follows from (27) that $\dot{z} \in \mathcal{L}_\infty$. Based on the fact that $z, \dot{z} \in \mathcal{L}_\infty$ and $z \in \mathcal{L}_2$, Barbalat's Lemma can be applied [33] to show that

$$\lim_{t \rightarrow \infty} z = 0. \quad (38)$$

Consequently, the clutch normal force tracking is also achieved by (20). For the convergence of adaptation parameters, the PE condition [34] has to be satisfied. If condition (28) in A4 holds, the PE condition is satisfied. Note that the $\hat{\phi}_1$ and $\hat{\phi}_2$ are utilized only for improving the motion tracking performance. The parameter for $\hat{r}(\hat{\mu})$ is only active when the clutch is engaged during the slip phase. It means that $\hat{r} \rightarrow r$ in $\Omega_\mu \times \Omega_{\hat{r}}$.

Finally, since the purpose of this scheme is the good estimation of the friction coefficient μ , it is required to derive an equation to estimate $\hat{\mu}$ from \hat{r} . The time derivative of \hat{r} can be obtained from (25) as

$$\dot{\hat{r}} = w \frac{d}{dt} \left(\frac{\hat{k}_b}{\hat{k}_b + k_a} \right) = w \frac{k_a}{(\hat{k}_b + k_a)^2} \dot{\hat{k}}_b. \quad (39)$$

The equation for $\dot{\hat{k}}_b$ is rewritten as

$$\dot{\hat{k}}_b = \frac{(\hat{k}_b + k_a)^2}{wk_a} \dot{\hat{r}} \quad (40)$$

where k_b is defined as a function of μ in (15a) for the notational simplicity. The estimated parameter of k_b and its time derivative are

$$\hat{k}_b = \hat{\xi}(\hat{\mu})(k_p \beta) \quad (41)$$

$$\dot{\hat{k}}_b = -(k_p R_c \beta) \dot{\hat{\mu}}. \quad (42)$$

Combining (40) and (42) yields

$$\dot{\hat{\mu}} = -\frac{(\hat{k}_b + k_a)^2}{wk_a k_p R_c \beta} \dot{\hat{r}}. \quad (43)$$

The adaptation law in terms of $\hat{\mu}$ is given by

$$\dot{\hat{\mu}} = -\frac{\{\hat{\xi}(\hat{\mu})(k_p \beta) + k_a\}^2}{wk_a k_p R_c \beta} \dot{\hat{r}}. \quad (44)$$

To guarantee the boundedness of parameter estimates, the projection operator is used at each step. The relationship from (39) to (44) concludes that $\hat{k}_b \rightarrow k_b$. Hence, the unknown parameter $\hat{\mu}$ also converges to an actual parameter μ in $\Omega_\mu \times \mathcal{P}_\mu$. ■

D. Disturbance Compensation by the DOB

In order to enhance control robustness, a DOB is incorporated with the adaptive sliding control developed in the previous subsection. The DOB estimates the lumped disturbances d_l defined in (18) and (19e) by using a low-pass filter $Q(s)$ and a nominal model [35]–[37]. After plugging this estimated disturbance into the control input, the uncertain plant behaves like the nominal model. The DOB-based control has advantages that it can effectively eliminate unstructured uncertainty under the specified passband of $Q(s)$.

The actuator position control for clutch applications requires a short settling time. The use of the larger feedback gain is limited particularly due to the actuator saturation. Therefore, the disturbance rejection capability is necessary to have the motor control bandwidth increased as much as possible through the accurate feedforward control. The DOB-based control is incorporated to improve the robustness to matched uncertainties d_l at

a low-frequency range, while the adaptive sliding control plays the role in dealing with structured uncertain parameter compensation in the high-frequency parts. The conventional DOB for linear systems [35] is modified for our nonlinear system.

The nominal system is denoted as $P_n : u_n \rightarrow \theta_m$, which can be obtained from neglecting the unknown disturbance d in the uncertain nonlinear system (18)

$$P_n : \bar{J}_m \dot{\omega}_m + q\omega_m + T_f(\omega_m) + r(\mu)\theta_m = pu_n \quad (45)$$

where u_n is the nominal control input. Note that u_n can be computed from numerically solving (45) inversely ($P_n^{-1} : \theta_m \rightarrow u_n$) with given initial conditions $\theta_m(0)$ and $\omega_m(0)$, and measurements θ_m and ω_m . Motivated from the conventional DOB [35], unknown disturbance d_l is approximated as the difference between the nominal input and the actual control input denoted by $d_l(z) \approx u_n - u$. Hence, \hat{d}_l is given by

$$\hat{d}_l = Q(s)d_l = Q(s)[u_n - u]. \quad (46)$$

Since $Q(s)$ is a stable low-pass filter, (46) can be rewritten by

$$\tau_q \dot{\hat{d}}_l = -\hat{d}_l + d_l, \quad \hat{d}_l(0) = 0 \quad (47)$$

where τ_q is a small parameter to adjust the passband of (47). The following theorem shows the boundedness and convergence of the unstructured disturbance estimator-based control incorporating the ASMC proposed in Theorem 1.

Theorem 2: Consider the case where the unstructured disturbance d_l is nonzero in the tracking error system (22). Given compact sets $\Omega_z \subset \mathbb{R}$ and $\Omega_{\tilde{d}_l} \subset \mathbb{R}$ of initial conditions $z(0)$ and $\tilde{d}_l(0)$, there exists $\tau_q^* > 0$ for all $0 < \tau_q < \tau_q^*$ and for all $z(0) \in \Omega_z$ and $\tilde{d}_l(0) \in \Omega_{\tilde{d}_l}$. The controller given by (23) in conjunction with the adaptation laws (30), (32), and (33) and the disturbance estimator (47) ensure

$$\tilde{\theta}_m \rightarrow 0, \quad \tilde{\mu} \rightarrow 0, \quad \text{and} \quad \tilde{d}_l \rightarrow 0 \quad \text{as} \quad t \rightarrow \infty$$

provided that the following inequalities are satisfied:

$$K > \frac{1}{2}, \quad \tau_q^* = \frac{1}{\frac{c_3^2}{2} + c_4}. \quad (48)$$

Proof: The disturbance estimation error at low frequencies is defined as $\tilde{d}_l = d_l - \hat{d}_l$. Using (47) and (27), the time derivative of \tilde{d}_l is given as

$$\dot{\tilde{d}}_l = -\frac{1}{\tau_q}\tilde{d}_l + \frac{\partial d_l(z)}{\partial z}\dot{z}. \quad (49)$$

Consider the Lyapunov function candidate $W(z, \tilde{d}_l) \in \mathbb{R}$ with V defined in (34)

$$W(z, \tilde{d}_l) = V(z, \tilde{r}, \tilde{\phi}_1, \tilde{\phi}_2') + \frac{1}{2}\tilde{d}_l^2. \quad (50)$$

The time derivative of (50) along the trajectory of (49) is given as

$$\begin{aligned} \dot{W}(z, \tilde{d}_l) &= \dot{V}(z, \tilde{r}, \tilde{\phi}_1, \tilde{\phi}_2') + \tilde{d}_l \dot{\tilde{d}}_l \\ &= -Kz^2 - p\tilde{d}_l z - \frac{1}{\tau_q}\tilde{d}_l^2 + \frac{\partial d_l(z)}{\partial z}\tilde{d}_l \dot{z} \end{aligned} \quad (51)$$

where the result of Theorem 1 is used for \dot{V} and the term $p\tilde{d}_l z$ is added for the case $d_l \neq 0$. Since the actuator is initially at rest, it follows that $\tilde{d}_l(0) = 0$ with $z(0) = 0$ in (49). It means that for any compact set Ω_z and $\Omega_{\tilde{d}_l}$ of $z(0)$ and $\tilde{d}_l(0)$, respectively, such a compact set can be found as

$$\Omega_z \times \Omega_{\tilde{d}_l} \subseteq \Omega_c. \quad (52)$$

In Theorem 1, (34) and (37) show that V is bounded. By the fact that z and the additional term from \tilde{d}_l are bounded, there exist $c_1 > 0$ and $c_2 > 0$ such that the inequalities

$$\dot{z} \leq c_1|z| + p|\tilde{d}_l| \quad (53)$$

$$\left| \frac{\partial d_l(z)}{\partial z} \right| \leq c_2 \quad (54)$$

hold on the level set Ω_c of W . Using (53) and (54), (51) is expressed as

$$\begin{aligned} \dot{W}(z, \tilde{d}_l) &\leq -Kz^2 - p\tilde{d}_l z - \frac{1}{\tau_q}\tilde{d}_l^2 + \tilde{d}_l \left| \frac{\partial d_l(z)}{\partial z} \right| [c_1|z| + p|\tilde{d}_l|] \\ &\leq -Kz^2 - \frac{1}{\tau_q}\tilde{d}_l^2 + c_3|z||\tilde{d}_l| + c_4\tilde{d}_l^2 \end{aligned} \quad (55)$$

$$\leq -Kz^2 - \frac{1}{\tau_q}\tilde{d}_l^2 + \frac{1}{2}z^2 + \frac{c_3^2}{2}\tilde{d}_l^2 + c_4\tilde{d}_l^2 \quad (56)$$

$$\leq -\left(K - \frac{1}{2}\right)z^2 - \left(\frac{1}{\tau_q} - \frac{c_3^2}{2} - c_4\right)\tilde{d}_l^2 \quad (57)$$

where $c_3 = c_1 c_2 - p$ and $c_4 = c_2 p$ with $c_1 c_2 > p$. By selecting (48), it can be concluded that there exists $0 < \tau_q < \tau_q^*$ such that \dot{W} is negative semidefinite on the level set Ω_c . The remaining part for parameter adaptation convergence can be stated by the similar way as in Theorem 1. ■

Remark 1: This approach is inspired from the conventional DOB. τ_q is a time constant of (47), which corresponds to the Q-filter parameter. The level set Ω_c defined in (52) implies the low-frequency range to be rejected by (46). From (48), it depends on the growth rate of disturbance with respect to the tracking error and the feedback gain K . Compared with the conventional DOB for linear systems, such a restriction is imposed for the extension to nonlinear systems. The block diagram of the closed-loop control system is shown in Fig. 4.

IV. EXPERIMENTAL VERIFICATION

A. Experimental Setup

The schematic of the overall control system architecture is shown in Fig. 5. Speed and torque sensor outputs are transferred to dSPACE MicroAutobox DS1401, which is a controller board for the rapid control prototyping system. For the purpose of feedback control, the motor position is measured using an incremental encoder with the resolution 0.026° per pulse that is attached at the back of the motor shaft. Note that the speed signal is obtained by pseudodifferentiation of the position measurement. The dc motor for the actuator is driven by an H-bridge driver, which provides pulse width modulated input. In addition, since the SECA system functions as a power transmission

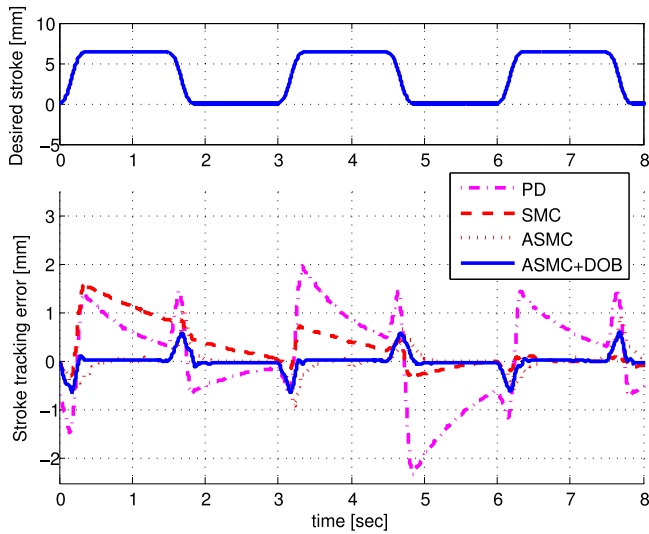


Fig. 6. Experimental results of the position tracking control in the clutch open phase (free space).

TABLE I
RMS POSITION TRACKING ERRORS AND THE MAXIMUM ERROR
FOR THE FOUR CASES

Controller type>	RMS error (mm)	Maximum error (mm)
PD	0.8188	2.2388
SMC	0.4300	1.5980
ASMC	0.2357	1.0937
ASMC+DOB	0.1752	0.6889

both controllers. However, it shows tracking errors during the transient period.

The ASMC-DOB shows that the tracking performance and robustness are effectively improved compared with other results. In this experiment, τ_q is selected as 0.016, which is 10-Hz Q-filter bandwidth. It can overcome the hysteretic motion friction and unmodeled effect. And, the settling time is reduced to 0.25 s, during which the clutch actuator stroke moves 3 mm away from free motion to clutch engagement. This is satisfactory for design specification of production vehicles. Therefore, experimental results confirm that the ASMC-DOB is the best candidate for the position control. The rms error and the maximum error are shown in Table I.

C. Clutch Engagement Control

The overall control strategy for clutch engagement has three modes: approaching, slip-ready, and engaging modes.

- 1) In the approaching mode, the clutch is initially at rest. The controller only considers the positioning work since the clutch is initially disengaged. Hence, the adaptation law (30) for $\hat{\mu}$ is not active and (32) and (33) are only activated.
- 2) When the clutch is positioned to the near contact point, this is called the slip-ready mode.
- 3) Then, the clutch is positioned to the desired stroke corresponding to the desired force for full engagement.

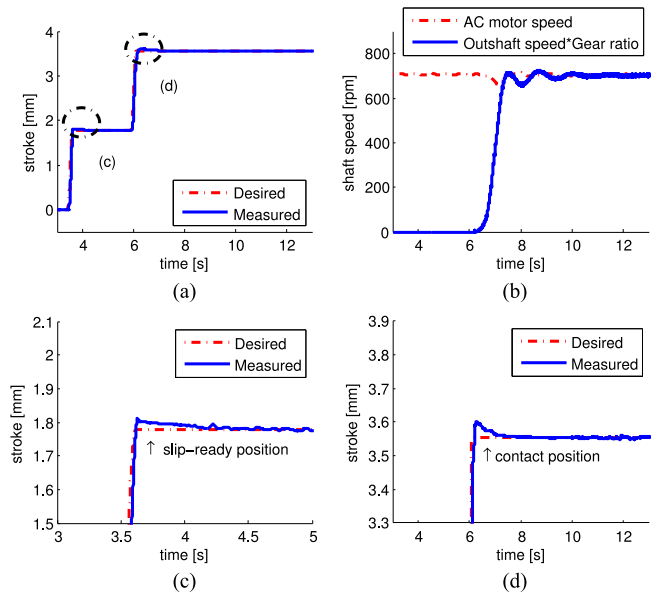


Fig. 7. Experimental results of the engagement control without adaptations. (a) Motor position (actuator stroke). (b) Input shaft (ac motor) and the output shaft speed. (c) Zoom of position response in the slip-ready position. (d) Zoom of position response in the contact position.

The clutch makes contact with the opposing surface from the near contact point. The adaptation law (30) is turned ON just in order to identify the disk friction coefficient. This is called the engaging mode. All modes utilize one position-based force control so that there is no switching phenomenon in transitions between each mode.

It is assumed that the stroke for the clutch to be engaged is known. This is a reasonable assumption since real vehicles generally have initial stroke search logic. The desired trajectory can be generated by the nonlinear filter [38] such that $\theta_{md}, \dot{\theta}_{md}, \ddot{\theta}_{md} \in \mathcal{L}_\infty$.

1) *Without Adaptations:* The actuator position control for engagement without adaptations has been conducted for comparison. Fig. 7(a) and (b) shows that the position tracking and the shaft speed synchronization are achieved well. In Fig. 7(c) and (d), the slip-ready position and the contact position in the engaging mode are magnified from Fig. 7(a). Although the desired actuator position is well tracked by the controller without any adaptation scheme, residual vibrations arise mainly due to the highly stiff contact.

2) *With Adaptations:* With the adaptation laws turned ON at each mode, the same experiments have been conducted. Fig. 8(a) shows that the actuator position can be controlled by the motor position. It shows that the clutch control starts with the clutch open phase, which corresponds to the approaching mode under the position control only. It can also be verified in Fig. 8(c). Approximately at 4 s, the clutch is moved into the near contact position and enters into the slip-ready mode. Then, once the engaging mode starts at 6 s, the clutch slip is reduced. Fig. 8(b) shows that two shaft speeds are synchronized.

Since the friction coefficient cannot be measured directly, the torque measurement from the torque sensor is utilized for verification. With these values, the disk friction coefficient is

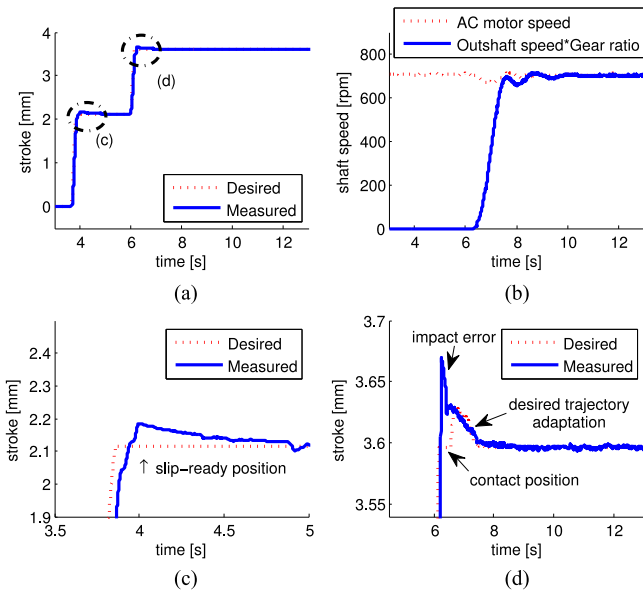


Fig. 8. Experimental results of ASMC-DOB. (a) Motor position (actuator stroke). (b) Input shaft (ac motor) and the output shaft speed. (c) Zoom of position response in the slip-ready position. (d) Zoom of position response in the contact position.

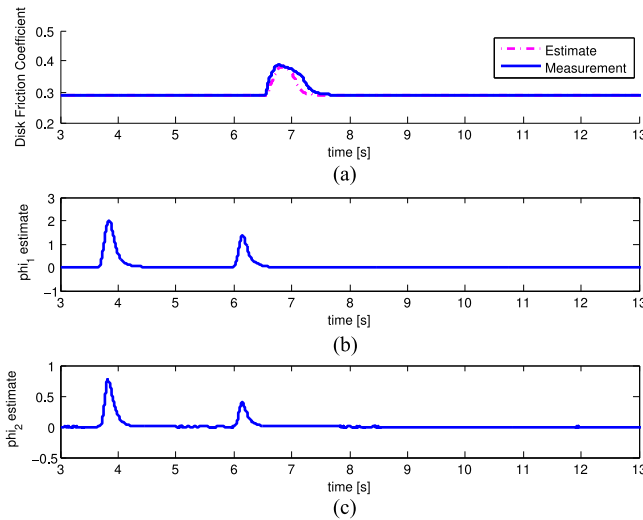


Fig. 9. Experimental results of ASMC-DOB. (a) Adaptation of the disk friction coefficient $\hat{\mu}$. (b) Adaptation results of motion friction parameters $\hat{\phi}_1$ and (c) $\hat{\phi}_2$.

obtained indirectly based on (6) incorporating the normal force, which depends on the actuator position. The friction coefficient μ on the disk is estimated as shown in Fig. 9(a). In this test, the friction coefficient $\hat{\mu}$ is initially set by 0.29. It was taken from the repeated experiment at the test bench. In Fig. 9(a), it is verified that the estimation $\hat{\mu}$ varies with the clutch slip speed.

Compared with the experimental measurement, it is shown that the proposed μ adaptation works reasonably well. The tracking error of the clutch normal force based on the position control can be compensated through the estimation of the friction coefficient on the disk. The closer look at the clutch contact from Fig. 8(a) can be found in Fig. 8(d), where the desired position is modified online as a function of the disk friction coefficient. It

can also be verified in (20) and Fig. 4. In Fig. 8(d), the peaking error occurs due to the transition effect from a free space to a stiff contact. This impact reaction may go beyond the DOB bandwidth specified by τ_q in (47). It should be noted that the disk friction coefficient $\hat{\mu}$ is estimated in the slip phase so that $\Phi(\hat{\mu})$ in (16) can be subsequently adapted as well.

In Fig. 8, tracking errors are observed due to the instantaneous contact impact. Figs. 8(d) and 9(a) show that $\hat{\mu}$ adaptation yields friction coefficient monitoring and engagement compensation simultaneously. In other words, while the disk friction coefficient is estimated, the desired position depending on the clutch normal force is also corrected at the same time. As a result, this adaptation scheme provides online stiffness inference for the clutch engagement control. Here, \hat{r} can be considered as the equivalent stiffness of the engagement force.

Fig. 9(b) and (c) shows the adaptation results of the motion friction parameters in the clutch actuator model. In particular, both parameters $\hat{\phi}_1$ and $\hat{\phi}_2$ are estimated in the dynamic regime of the clutch actuator positioning.

Remark 2: It should be noted that the test bench does not have any external damper to absorb residual vibrations of the drivetrain. Hence, this may impose the worst case for testing any clutch apparatus. If the system has a mass flywheel, the control quality of the engagement will be further improved significantly.

V. CONCLUSION

In this paper, the control strategy for a SECA system is developed based on ASMC with DOB compensation. The proposed adaptation algorithm considers not only parametric uncertainties but also robustness of the clutch engagement. The desired force is adjusted by monitoring the disk friction coefficient in real time. The experimental results show that the control performance can be improved significantly when the controller is combined with the parameter adaptation and the disturbance compensation. The proposed engagement control based on actuator position tracking can be used for the general clutch actuator systems in automotive applications as well as a SECA system.

REFERENCES

- [1] A. Serrarens, M. Dassen, and M. Steinbuch, "Simulation and control of an automotive dry clutch," in *Proc. Amer. Control Conf.*, Boston, MA, USA, 1999, vol. 5, pp. 4078–4083.
- [2] A. Heijden, A. Serrarens, M. Camlibel, and H. Nijmeijer, "Hybrid optimal control of dry clutch engagement," *Int. J. Control*, vol. 80, no. 11, pp. 1717–1728, 2007.
- [3] F. Garofalo, L. Glielmo, L. Iannelli, and F. Vasca, "Optimal tracking for automotive dry clutch engagement," in *Proc. IFAC 15th Triennial World Congr.*, Barcelona, Spain, 2002, pp. 367–372.
- [4] P. Dolcini, H. Bechart, and C. C. de Wit, "Observer-based optimal control of dry clutch engagement," in *Proc. 44th IEEE Conf. Dec. Control/Eur. Control Conf.*, Seville, Spain, Dec. 12–15, 2005, pp. 440–445.
- [5] P. Dolcini, C. C. de Wit, and H. Bechart, "Lurch avoidance strategy and its implementation in amt vehicles," *Mechatronics*, vol. 18, no. 56, pp. 289–300, 2008.
- [6] L. Glielmo and F. Vasca, "Engagement control for automotive dry clutch," in *Proc. Amer. Control Conf.*, Chicago, IL, USA, 2000, pp. 1016–1017.
- [7] J. Fredriksson and B. S. Egardt, "Nonlinear control applied to gearshifting in automated manual transmission," in *Proc. 39th IEEE Conf. Dec. Control*, Sydney, NSW, Australia, Dec. 2000, pp. 444–449.
- [8] B. Gao, H. Chen, K. Sanada, and Y. Hu, "Design of clutch-slip controller for automatic transmission using backstepping," *IEEE/ASME Trans. Mechatronics*, vol. 16, no. 3, pp. 498–508, Jun. 2011.

- [9] L. Chen, G. Xi, and C. Yin, "Model referenced adaptive control to compensate slip-stick transition during clutch engagement," *Int. J. Automot. Technol.*, vol. 12, pp. 913–920, 2011.
- [10] M. Pisaturo, M. Cirrincione, and A. Senatore, "Multiple constrained MPC design for automotive dry clutch engagement," *IEEE/ASME Trans. Mechatronics*, vol. 20, no. 1, pp. 469–480, Feb. 2015.
- [11] A. Myklebust and L. Eriksson, "Modeling, observability, and estimation of thermal effects and aging on transmitted torque in a heavy duty truck with a dry clutch," *IEEE/ASME Trans. Mechatronics*, vol. 20, no. 1, pp. 61–72, Feb. 2015.
- [12] J. Oh and S. Choi, "Real-time estimation of transmitted torque on each clutch for ground vehicles with dual clutch transmission," *IEEE/ASME Trans. Mechatronics*, vol. 20, no. 1, pp. 24–36, Feb. 2015.
- [13] J. Kim and S. B. Choi, "Nonlinear torque observer for a self-energizing clutch actuator using a reaction torque estimation approach," *IEEE/ASME Trans. Mechatronics*, vol. 20, no. 6, pp. 3071–3084, Dec. 2015.
- [14] F. Vasca, L. Iannelli, A. Senatore, and G. Reale, "Torque transmissibility assessment for automotive dry-clutch engagement," *IEEE/ASME Trans. Mechatronics*, vol. 16, no. 3, pp. 564–573, Jun. 2011.
- [15] J. Horn, J. Bamberg, P. Michaub, and S. Pindlb, "Flatness-based clutch control for automated manual transmissions," *Control Eng. Pract.*, vol. 11, pp. 1353–1359, 2003.
- [16] G. Lucente, M. Montanari, and C. Rossi, "Modelling of an automated manual transmission system," *Mechatronics*, vol. 17, pp. 73–91, 2007.
- [17] M. Montanari, F. Ronchi, C. Rossi, A. Tili, and A. Tonielli, "Control and performance evaluation of a clutch servo system with hydraulic actuation," *Control Eng. Pract.*, vol. 12, pp. 1369–1379, 2004.
- [18] S. Li, C. Wu, and Z. Sun, "Design and implementation of clutch control for automotive transmissions using terminal-sliding-mode control and uncertainty observer," *IEEE Trans. Veh. Technol.*, vol. 65, no. 4, pp. 1890–1898, Apr. 2016.
- [19] F. Meng, H. Zhang, D. Cao, and H. Chen, "System modeling and pressure control of a clutch actuator for heavy-duty automatic transmission systems," *IEEE Trans. Veh. Technol.*, vol. 65, no. 7, pp. 4865–4874, Jul. 2016.
- [20] X. Song and Z. Sun, "Pressure-based clutch control for automotive transmissions using a sliding-mode controller," *IEEE/ASME Trans. Mechatronics*, vol. 17, no. 3, pp. 534–546, Jun. 2012.
- [21] H. Langjord, T. Johansen, and J. Hespanha, "Switched control of an electropneumatic clutch actuator using on/off valves," in *Proc. Amer. Control Conf.*, Jun. 2008, pp. 1513–1518.
- [22] H. Langjord and T. Johansen, "Dual-mode switched control of an electropneumatic clutch actuator," *IEEE/ASME Trans. Mechatronics*, vol. 15, no. 6, pp. 969–981, Dec. 2010.
- [23] B. Gao, H. Chen, Q. Liu, and H. Chu, "Position control of electric clutch actuator using a triple-step nonlinear method," *IEEE Trans. Ind. Electron.*, vol. 61, no. 12, pp. 6995–7003, 2014.
- [24] L. Li, X. Wang, X. Qi, X. Li, D. Cao, and Z. Zhu, "Automatic clutch control based on estimation of resistance torque for AMT," *IEEE/ASME Trans. Mechatronics*, vol. 21, no. 6, pp. 2682–2693, Dec. 2016.
- [25] J. Kim and S. B. Choi, "Self-energizing clutch actuator system: Basic concept and design," in *Proc. World Automot. Congr.*, May 2010, Art. no. FISITA2010-SC-P-23.
- [26] J. Kim and S. B. Choi, "Design and modeling of a clutch actuator system with self-energizing mechanism," *IEEE/ASME Trans. Mechatronics*, vol. 16, no. 5, pp. 953–966, Oct. 2011.
- [27] J. Kim and S. B. Choi, "Adaptive force control of automotive clutch actuator system with self-energizing effect," in *Proc. 18th IFAC World Congr.*, Milano, Italy, Aug. 2011, pp. 5088–5093.
- [28] Y. Cao and X. B. Chen, "Disturbance-observer-based sliding-mode control for a 3-DoF nanopositioning stage," *IEEE/ASME Trans. Mechatronics*, vol. 19, no. 3, pp. 924–931, Jun. 2014.
- [29] Y. Lee, S. H. Kim, and C. C. Chung, "Integral sliding mode control with a disturbance observer for next-generation servo track writing," *Mechatronics*, vol. 40, pp. 106–114, Dec. 2016.
- [30] Z. J. Yang, S. Hara, S. Kanae, K. Wada, and C. Y. Su, "An adaptive robust nonlinear motion controller combined with disturbance observer," *IEEE Trans. Control Syst. Technol.*, vol. 18, no. 2, pp. 454–462, Mar. 2010.
- [31] C. D. Wit, H. Olsson, K. Astrom, and P. Lischinsky, "A new model for control of systems with friction," *IEEE Trans. Automat. Control*, vol. 40, no. 3, pp. 419–425, Mar. 1995.
- [32] V. Utkin, J. Guldner, and J. Shi, *Sliding Mode Control in Electromechanical Systems*. New York, NY, USA: Taylor & Francis, 1999.
- [33] J. J. E. Slotine and W. Li, *Applied Nonlinear Control*. Englewood Cliffs, NJ, USA: Prentice-Hall, 1991.
- [34] S. Sastry and M. Bodson, *Adaptive Control, Stability, Convergence and Robustness*. Englewood Cliffs, NJ, USA: Prentice-Hall, 1989.
- [35] K. Ohnishi, "A new servo method in mechatronics," *Trans. Jpn. Soc. Elect. Eng.*, vol. 107, no. D, pp. 83–86, 1987.
- [36] T. Umeno, T. Kaneko, and Y. Hori, "Robust servosystem design with two degrees of freedom and its application to novel motion control of robot manipulators," *IEEE Trans. Ind. Electron.*, vol. 40, no. 5, pp. 473–485, Oct. 1993.
- [37] B. K. Kim and W. K. Chung, "Advanced disturbance observer design for mechanical positioning systems," *IEEE Trans. Ind. Electron.*, vol. 50, no. 6, pp. 1207–1216, Dec. 2003.
- [38] R. Zanasi, C. L. Bianco, and A. Tonielli, "Nonlinear filters for the generation of smooth trajectories," *Automatica*, vol. 36, no. 3, pp. 439–448, 2000.



Jinsung Kim (S'10–M'13) received the Ph.D. degree in mechanical engineering from the Korea Advanced Institute of Science and Technology, Daejeon, South Korea, 2013.

In 2013, he joined the Division of Research and Development, Hyundai Motor Company, Hwasung, South Korea, where he is currently a Senior Research Engineer working on the development of powertrain control software. He designed clutch control algorithms of a seven-speed dual-clutch transmissions for production vehicles. His current research interests include automotive systems, nonlinear control, observer design, and integrated design and control of complex mechanical systems.



Seibum B. Choi (M'09) received the B.S. degree in mechanical engineering from Seoul National University, Seoul, South Korea, in 1985, the M.S. degree in mechanical engineering from the Korea Advanced Institute of Science and Technology (KAIST), Daejeon, South Korea, in 1987, and the Ph.D. degree in control from the University of California, Berkeley, CA, USA, in 1993.

From 1993 to 1997, he was involved in the development of automated vehicle control systems at the Institute of Transportation Studies, University of California. In 2006, he was at TRW, Livonia, MI, USA, where he was involved in the development of advanced vehicle control systems. Since 2006, he has been a Faculty Member with the Department of Mechanical Engineering, KAIST. His current research interests include fuel-saving technology, vehicle dynamics and control, and active safety systems.



Jiwon J. Oh received the B.S., M.S., and Ph.D. degrees in mechanical engineering from the Korea Advanced Institute of Science and Technology, Daejeon, South Korea, in 2009, 2012, and 2016, respectively.

He is currently a Senior Research Engineer with Hyundai Motor Company, Hwasung, South Korea. His research interests include vehicle driveline state estimation and hybrid powertrain clutch control.